

JOURNAL OF ADVANCED APPLIED SCIENCES

PRENSIP
https://prensip.gen.tr

e-ISSN: 2979-9759

RESEARCH ARTICLE

New Crystal Photodiode Combination for Environmental Radiation Measurement

Ilhan Tapan¹™ • Fatma Kocak² •

¹Aksaray University, Faculty of Science and Letters, Department of Physics, Aksaray/Türkiye ²Bursa Uludağ University, Faculty of Science and Letters, Department of Physics, Bursa/Türkiye

ARTICLE INFO

Article History

Received: 26.10.2023 Accepted: 21.11.2023 First Published: 18.12.2023

Keywords

Environmental radiation Radiation measurement Scintillation crystals ZnS–Si photodiodes



ABSTRACT

Here, a new design will be introduced to detect radiation in the environment with high efficiency. The designed structure consists of placing ZnS–Si APD and PIN photodiodes at the ends of conventional crystals such as NaI(Tl) and CsI(Tl). Since ZnS is transparent to photons with wavelengths between 340 and 10000 nm, photons coming from the crystals are absorbed directly in the depletion region and generate primary particles. With an increase in the number of generated primary particles, a stronger and cleaner signal is obtained. In the simulation work, the light generated by 30 keV–3 MeV gamma rays in the crystals was obtained using the Geant4 simulation code. The single-particle Monte Carlo technique was used to calculate the photodiode output signal for the crystal emission spectrum. The simulation results showed that the crystals and ZnS–Si photodiode structures formed a good combination. The high quantum efficiency and low excess noise factor make the ZnS–Si structure an excellent choice for scintillating light detection.

Please cite this paper as follows:

Tapan, I., & Kocak, F. (2023). New crystal photodiode combination for environmental radiation measurement. *Journal of Advanced Applied Sciences*, 2(2), 64-67. https://doi.org/10.61326/jaasci.v2i2.103

1. Introduction

Environmental radiation is also called "background radiation" because it is the radiation that exists all around us. The source of this radiation may be natural or man-made artificial radiation. Although the annual environmental radiation dose varies depending on location, the exposure from artificial radiation is around 2.3 mSv/year, whereas the exposure from natural radiation is around 1.5 mSv/year. Highly received radiation doses may cause serious health problems. Therefore, it is important to measure environmental radiation values easily and practically. There are many studies in the literature for this purpose, such as (Lowder & Condon, 1965;

Sáez-Vergara, 2000; Koyama et al., 2010; Lowdon et al., 2019; Zhang et al., 2022).

2. Materials and Methods

The environmental dose rate is obtained by measuring γ -rays in the air. There are several types of detector combinations to detect radiation. Commercially available radiation detectors are available for measuring environmental radiation. For example, there are compact radiation detection modules based on CsI(Tl) and SiPM that can be used for gamma counting and energy measurements produced by The Hamamatsu Photonics (2023). This product basically consists of a crystal

[™] Correspondence

E-mail address: ilhantapan@aksaray.edu.tr



photodetector combination. In this combination, a photodiode (PD) and photomultiplier tube (PMT) can also be used as the photodetector.

The structure we propose for detecting environmental radiation is a crystal photodetector combination. In this structure, the photons generated from incident gamma rays in the crystal are detected from the photodiodes placed at the rear end of the crystals (Figure 1).

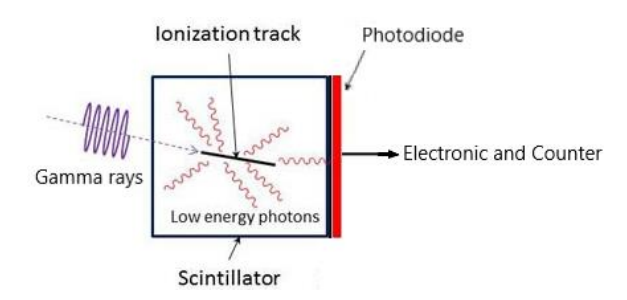


Figure 1. Sketch of a crystal photodetector combination.

The designed structure consists of conventional crystals such as NaI(Tl) or CsI(Tl) and a ZnS–Si avalanche photodiode. Crystals are commonly used for radiation measurements and are easily available from the market. As the NaI(Tl) crystal emits light in the wavelength region from 340 to 520 nm peaking at around 410 nm, the CsI(Tl) crystal emits light in the wavelength region from 380 to 720 nm, peaking at around 530 nm. The scintillation light emission spectra of the crystals are given in Figure 2.

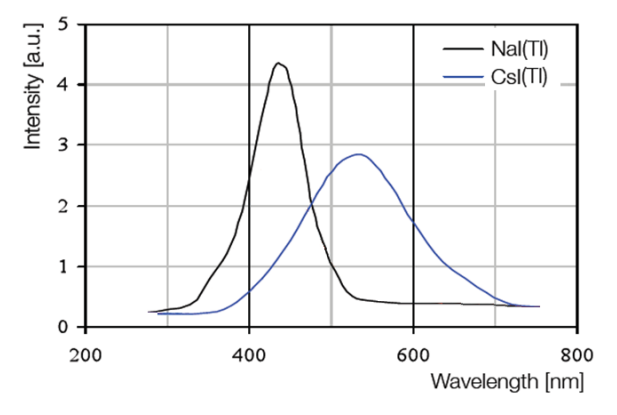


Figure 2. Scintillation light emission spectra of NaI(Tl) and CsI(Tl) crystals.

The photodetector should be sensitive to light coming from the crystals. For this reason, the Zinc Sulfide (ZnS) – Silicon (Si) avalanche photodiode (APD) is proposed. The ZnS–Si isotype hetero-junction APD structure consists of successive layers of p⁺-type ZnS, p-type Si, n-type Si, n⁻-type Si, and n⁺-type Si semiconductors with thicknesses of 3, 6, 5, 20 and 3 mm, respectively. Figure 3 shows the ZnS-Si APD structure and the electric field distribution inside the detector.

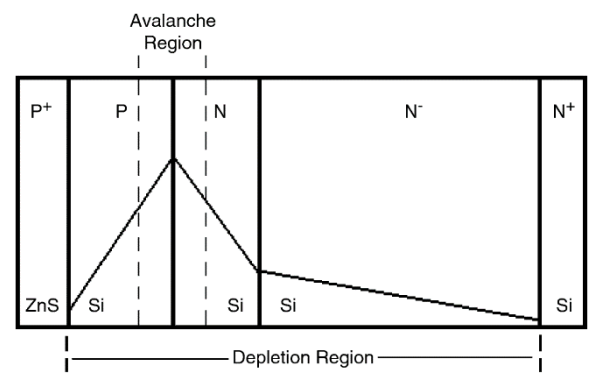


Figure 3. Sketch of the ZnS–Si isotype heterojunction avalanche photodiode structure.

ZnS has the photon absorption edge at approximately 340 nm, which corresponds to an energy band gap of 3.68 eV, and has a transparency region until approximately 10,000 nm. This makes the ZnS–Si APD structure has very high quantum efficiency for photons of wavelength in the region from 340 nm to 800 nm (Figure 4). At longer wavelengths greater than 800 nm, some parts of the photons penetrate well into the APD depletion region and are absorbed in the $\rm n^+$ layer. This instance causes a decrease in the detector quantum efficiency (Tapan et al., 2006).

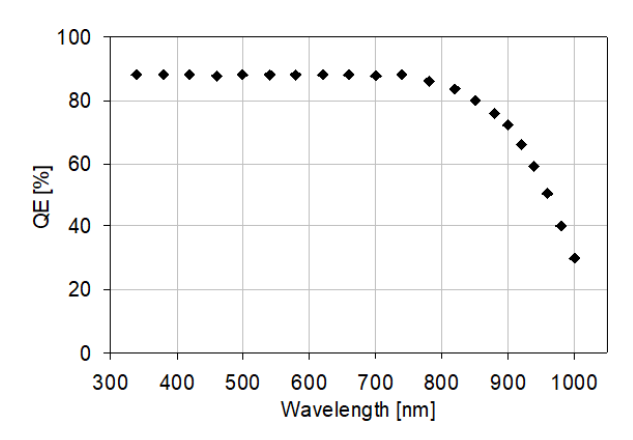


Figure 4. Quantum efficiency as a function of wavelength for the ZnS–Si APD structures.

Incident photons with wavelengths greater than 340 nm easily penetrate the ZnS surface layer, create electron-hole pairs in the Si depletion layer, and produce a detectable signal. Thus, the ZnS–Si avalanche photodiode structure is suitable for Nal(Tl) and CsI(Tl) photons due to its high quantum efficiency at small wavelengths.

3. Simulation and Results

Two simulation codes were used in the simulation works: Geant4 and Monte Carlo (M.C.) Fortran codes, as illustrated in Figure 5. In the first part of the simulation, the generation of scintillation light within the crystals by 30 keV-3 MeV incident gamma rays was performed using the Geant4 simulation code (The Geant4, 2023). In the second part of the simulation, the

light generated in the crystals is detected by the ZnS–Si APD placed at the end of the crystals. The signal generation process was performed by tracking a large number of individual scintillation photons coming from the crystals and following the generated charge carries through the well-defined ZnS–Si APD geometry using the single-particle M. C. simulation code written in Fortran.

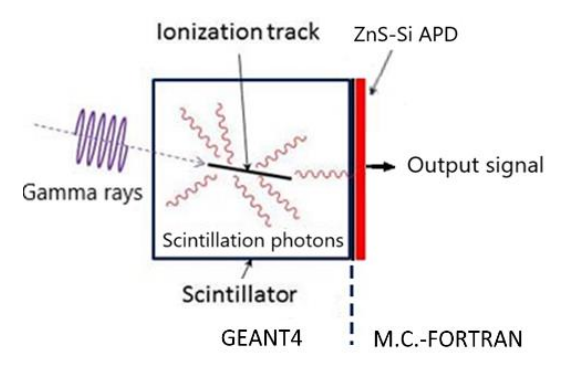


Figure 5. Parts of the simulation: The energy deposition and scintillation light generation in the crystal by Geant4 is the first part. Signal generation process by the M.C. Fortran in the detector is the second part.

Gamma rays were sent to the 5 cm diameter crystals with a cylindrical geometry, and their energy deposition inside the crystal was obtained. As an example, Figure 6 shows the Geant4 simulation of the energy deposition of 3 MeV energy gamma rays sent into an 8 cm long NaI(Tl) crystal.

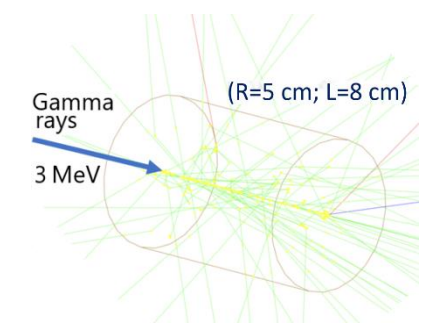


Figure 6. Geant4 simulation of energy deposition in the crystal.

The simulation was repeated by sending gamma rays between 30 keV and 3 MeV to the crystals of different lengths. The results were plotted and can be seen in Figure 7.

At lower energies, most of the gammas are absorbed and their energies are deposited. Increasing the incident gamma energy, the number of gammas escaping without interacting within the crystal increases, so the full energy deposition within the crystal decreases. It can also be seen from the figure that the deposited energy in the crystal increases as the crystal length increases.

The same simulation works were repeated for the CsI(Tl) crystal, and the results were plotted in Figure 8. As the CsI(Tl) crystal has a smaller radiation length than the NaI(Tl) crystal,

more energy depositions were obtained at the same crystal dimensions.

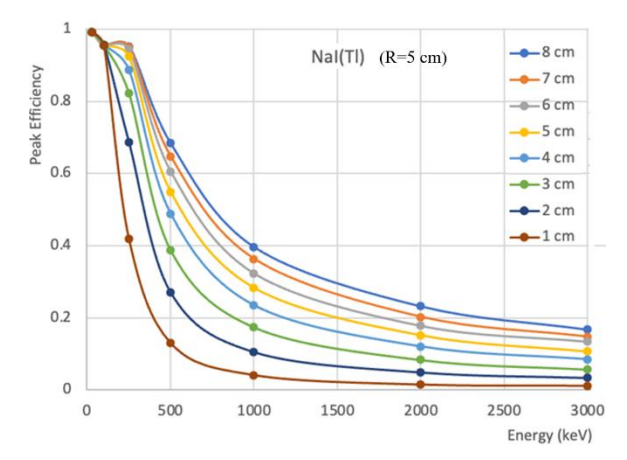


Figure 7. Variation of full energy deposition efficiency with incident gamma energies at different NaI(Tl) crystal sizes.

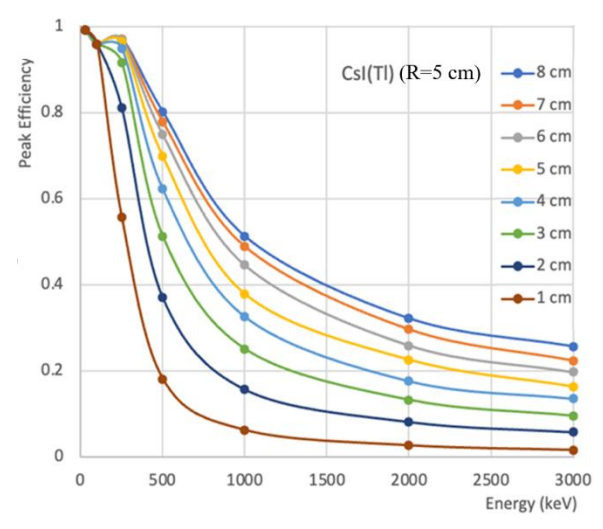


Figure 8. Variation of full energy deposition efficiency with incident gamma energies at different CsI(Tl) crystal sizes.

As a result of the energy deposition in the crystals, scintillation photons are emitted in the range of the emission spectra shown in Figure 2. ZnS–Si APD output signals for photons emitted in accordance with the emission spectra of the crystals were obtained using the M.C. Fortran code. Figure 9 shows the simulated output charge signal distributions of the ZnS–Si APD structure for the NaI(Tl) photons generated by gammas at different energies.

Even high-energy gammas escape, they still deposit more energy in the crystal and produce more scintillation light. Thus, more scintillation photons generated at higher gamma energies give clear signals.

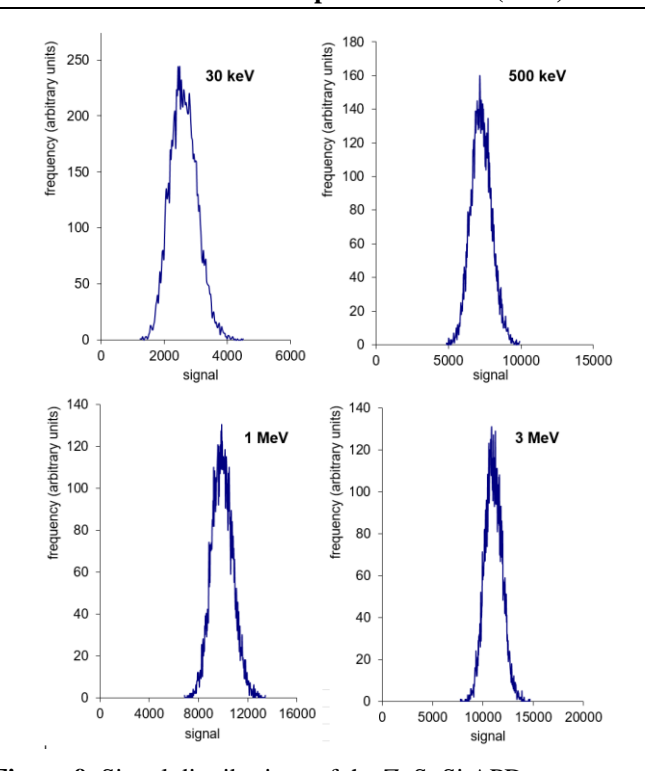


Figure 9. Signal distributions of the ZnS-Si APD structure.

4. Discussion

NaI(Tl) and CsI(Tl) crystals emit scintillation photons at short wavelengths, and some of these photons can be absorbed before being detected by the photodetector, resulting in the loss of photons. The loss can be prevented by using the ZnS–Si APD structure as a photodetector. Since ZnS is transparent to photons with wavelengths between 340 and 10000 nm, incoming photons in this wavelength range are absorbed directly in the depletion region and generate primary particles. With the increase in the number of generated primary particles, a stronger and cleaner signal can be obtained.

5. Conclusion

The simulation results showed that the crystals and ZnS–Si photodiode structures formed a good combination. The high quantum efficiency makes the ZnS–Si structure an excellent choice for both NaI(Tl) and CsI(Tl) scintillating light detection. This combination provides efficient detection for environmental radiation measurements.

Conflict of Interest

The authors declare that they have no conflict of interest.

References

- Koyama, S., Miyamoto, Y., Fujiwara, A., Kobayashi, H., Ajisawa, K., Komori, H., Takei, Y., Nanto, H., Kurobori, T., Kakimoto, H., Sakakura, M., Shimotsuma, Y., Miura, K., Hirao, K., & Yamamoto, T. (2010). Environmental radiation monitoring utilizing solid state dosimeters. *Sensors and Materials*, 22(7), 377-385.
- Lowder, W. M., & Condon, W. J. (1965). Measurement of the exposure of human populations to environmental radiation. *Nature*, 206(4985), 658-662.
- Lowdon, M., Martin, P. G., Hubbard, M. W. J., Taggart, M. P., Connor, D. T., Verbelen, Y., Sellin, P. J., & Scott, T. B. (2019). Evaluation of scintillator detection materials for application within airborne environmental radiation monitoring. *Sensors*, *19*(18), 3828-3841. https://doi.org/10.3390/s19183828
- Sáez-Vergara, J. C. (2000). Recent developments of passive and active detectors used in the monitoring of external environmental radiation. *Radiation Protection Dosimetry*, 92(1), 83-88. https://doi.org/10.1093/oxfordjournals.rpd.a033289
- Tapan, I., Ahmetoglu, M. A., & Kocak, F. (2006). A ZnS—Si isotype heterojunction avalanche photodiode structure for scintillation light detection. Nuclear Instruments and Methods in Physics Research A: Accelerators, Spectrometers, Detectors and Associated Equipment, 567(1), 268-271. https://doi.org/10.1016/j.nima.2006.05.105
- The Geant4. (2023). *The Geant4 simulation code*. Geant4 A Simulation Toolkit. https://geant4.web.cern.ch/
- The Hamamatsu Photonics. (2023). *Radiation sensors*. Hamamatsu. https://www.hamamatsu.com/eu/en/product/optical-sensors/radiation-sensor.html
- Zhang, J., Xiang, Y., Wang, C., Chen, Y., Tjin, S. C., & Wei, L. (2022). Recent advances in optical fiber enabled radiation sensors. *Sensors*, 22(3), 1126-1149. https://doi.org/10.3390/s22031126